Microsolvation–Induced Quantum Localization in Protonated Methane

Alexander Witt, Sergei D. Ivanov,* and Dominik Marx
Lehrstuhl für Theoretische Chemie, Ruhr-Universität Bochum, 44780 Bochum, Germany
(Received 24 August 2012; published 21 February 2013)

Nuclear quantum effects are responsible for vivid large-amplitude motion in protonated methane CH_5^+, which enables so-called "hydrogen scrambling" that leads to the dynamical equivalence of all five protons even at low temperatures. But what is the impact of external perturbations on hydrogen scrambling of CH_5^+ in this quantum fluxional ground state? We report *ab initio* path integral simulations of $CH_5^+(H_2)_n$, $n = 1, 2, 3$ that demonstrate cessation of hydrogen scrambling at low temperatures (20 K), but only slowdown at moderate temperatures (110 K). Importantly, different and unexpected mechanisms that are responsible for freezing the scrambling dynamics are revealed and traced back to distinct microsolvation patterns.

DOI: 10.1103/PhysRevLett.110.083003 PACS numbers: 31.15.xv, 31.15.xk, 36.40.Wa, 82.40.Qt

Protonated methane, CH_5^+, being a prototypical "nonclassical" molecule, is relevant to a wide range of fields such as plasma or astrophysics to name but two [1]. The properties of this enigmatic molecule, as opposed to its quasirigid parent CH_4 (methane), are governed by large-amplitude motion as a result of an unusually flat potential energy landscape with many (quasi) degenerate minima. At the fundamental level, most intriguing is the fact that large-amplitude motion leads to the dynamical equivalence of all five protons dubbed "hydrogen scrambling," which has been clarified in the last two decades only due to an intimate interplay of vibrational spectroscopy and computer simulation [2–13]. In particular, *ab initio* path integral (AIPI) simulations have shown that nuclear quantum effects override freezing upon lowering the temperature, which renders the molecule fully fluxional in its quantum ground state [4,7,8]. Furthermore, laser-induced reaction spectroscopy in combination with *ab initio* molecular dynamics (AIMD) [9,14] has demonstrated "full scrambling" at finite temperatures, here ~100 K, not only for CH_5^+ but for all its H/D isotopes [7,13,15].

What happens, however, if quantum fluxional CH_5^+ gets perturbed, e.g., by attaching small species as required in action spectroscopy, using "messengers" such as H_2, CH_4, or Ar? Apart from understanding how the properties of CH_5^+ itself get affected by the messengers, this raises the basic question about the competition of quantum fluxionality, leading to delocalization, and microsolvation, favoring localization due to weak intermolecular interactions, which is at the heart of this study. Various messenger species [16–18] have been attached to CH_5^+ in an attempt to indirectly characterize its structure. In this vein, pioneering messenger vibrational spectroscopy [19–21] by the group of Y. T. Lee employed n H_2 messengers to reveal clear signatures of microsolvation effects depending on n in the action spectra for the part of C-H stretching band recorded. In conjunction with AIMD simulations, this led to the final conclusion: "The complete freezing of the scrambling motions was found when the first three H_2 molecules were bound to the CH_5^+ core" [21]. Unfortunately, the spectra have been reported only in a quite limited frequency window which makes any firm assignment difficult. More importantly, the nuclei in the AIMD simulations have been treated by classical mechanics at a temperature of 100 K, a simulation setup at which scrambling is frozen even without attaching any H_2 molecules [22]. Since quantum effects clearly dominate the dynamics of bare CH_5^+ at low temperatures leading to a quantum fluxional ground state, it is anticipated that they play also a highly important role when assessing the impact of microsolvation. Using full quantum simulations at two temperatures relevant to the aforementioned experiment and to the ground state, we unravel an unexpectedly intricate interplay of quantum fluxionality and microsolvation which depends most sensitively on the number n of attached messengers.

CH_5^+ *structure*.—The equilibrium structure of CH_5^+, which is of eclipsed e-C_s symmetry consists of two structural entities: CH_3 "tripod" (atom C, and the H atoms labeled as 3, 4, and 5) and H_2 "moiety" (H atoms 1 and 2); see left inset (a) in Fig. 1 where H atoms 1, 2, and 3 and C constitute the symmetry plane. Full hydrogen scrambling can only occur upon two internal rearrangements. One is internal rotation of the H_2 moiety, with respect to the pseudo-C_3 axis of the CH_3 tripod via a staggered s-C_s saddle point, and the other is based on breaking apart the moiety and forming a new moiety by atoms 2 and 3 via a C_{2v} saddle point [see right inset (b) in Fig. 1 where C and H atom 2 form the rotation axis, whereas atoms 2, 4, 5 and C constitute the second symmetry plane] involving barriers of only ≈ 50 K and 400 K, respectively [14]. The former process is referred to as "internal rotation" while the latter is dubbed "partial scrambling." Importantly, only the combination of the two enables large-amplitude motion and thus "full scrambling," which allows all protons to visit all sites in the molecular frame thus rendering CH_5^+

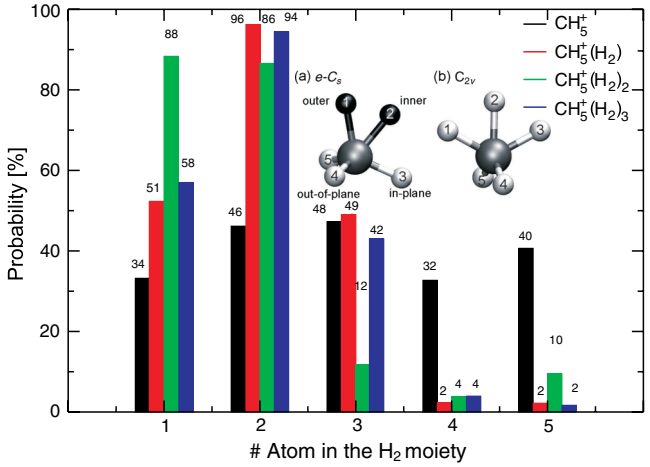

FIG. 1 (color online). Probabilities for atoms to participate in the moiety in CH_5^+ (black), $CH_5^+(H_2)$ (red), $CH_5^+(H_2)_2$ (green), and $CH_5^+(H_2)_3$ (blue) at $T = 20$ K. Insets (a) and (b) visualize the relevant structures e-C_s and C_{2v}, respectively. The labeling of atoms is arbitrary but fixed by using that of the initial structure for reference as defined in the insets (a) and (b): #1 outer, #2 inner, #3 in-plane, and #4 and #5 out-of-plane atoms.

fully fluxional, whereas partial scrambling leads to the well-known small-amplitude motion only.

Methods.—The Kohn-Sham density functional theory in the generalized gradient approximation as implemented in the CPMD program package [23] has been used for all *ab initio* simulations [24]. When it comes to calculations of CH_5^+ microsolvation complexes, there is only very scarce information available [25–27]. In order to account for correct binding energies, Grimme's dispersion correction [28] was added to the LDA + B functional, which has been used so far by us [4,7,9,13–15]. The accuracy of this LDA + B + D setup has been carefully validated [29] against available basis-set extrapolated CCSD(T) and MP2 benchmark data [27]; these findings are recapitulated in the Supplemental Material [30]. For all simulations, a cubic 25 a.u. box was used with a plane wave cutoff of 35 Ry. AIPI simulations [24] were performed at $T = 110$ K employing $P = 32$ replica and a formal time step of about 0.3 fs, while at 20 K the number of beads was increased to 128 to preserve convergence; the trajectory length corresponds formally to about 60 ps for each and every case. Note that we aimed exclusively at analyzing the impact of quantum effects on structure where AIPI methods are exact for $P \to \infty$. Importantly, nuclear spin effects stemming from Fermi-Dirac statistics are expected to be negligible; therefore, the nuclei are treated as distinguishable (Boltzmann) particles [13,31]. In order to prevent H_2 molecules from being thermally detached during long simulations, a harmonic restraining potential has been applied.

Results.—We have first performed AIPI simulations for bare CH_5^+ and the microsolvated species with up to three solvating H_2 molecules at a moderate temperature of $T = 110$ K, being close to that of spectroscopic studies [9,13,20,21]. At this temperature, the number of partial scrambling events is found to decrease by roughly one third after microsolvating CH_5^+ by three H_2 molecules, indicating that hydrogen scrambling is slowed down but definitively not stopped, as proposed earlier [20,21]. Note that the H_2 moiety is vividly rotating at 110 K, which implies that partial scrambling leads to full scrambling. This impact of microsolvation on scrambling cannot be an electronic structure effect since it has been shown that the barrier for partial scrambling is even decreased upon solvation [27,29] with H_2, and thus cannot be responsible for the observed slowdown upon microsolvating CH_5^+.

This raises the question if it is possible at all to fully stop hydrogen scrambling in microsolvated CH_5^+ and thus to localize its structure. In order to answer this question, we performed AIPI simulations at a sufficiently low temperature of 20 K where quantum effects are dominant and the thermal energy is too low to overcome the partial scrambling barrier [22]. Therefore, if hydrogen scrambling cannot be stopped at this temperature, then, most likely, it cannot be stopped at all. It turned out that while bare CH_5^+ remains fully fluxional in accord with the earlier results [4], full scrambling is suppressed for any microsolvated CH_5^+ species at this temperature. This is a central observation which underlies the subsequent mechanistic analysis of how quantum large-amplitude motion and microsolvation compete at low temperatures.

Site-specific analysis.—It follows from static calculations [27] that the first solvating H_2 molecule preferentially attaches to the inner atom, the second one to the outer atom, followed by the third H_2 which attaches to the in-plane atom, see inset (a) in Fig. 1 for this nomenclature, whereas other solvation patterns turn out to be noticeably higher in energy. The same solvation patterns are dominant in the full quantum simulations. In order to track scrambling in AIPI, we determined the moiety in each replica (imaginary time slice) along the AIPI trajectories separately, which enables one to identify different structural subunits. The respective probabilities for atoms to constitute the moiety are shown in Fig. 1; note that since the nuclei are treated as distinguishable particles, they can be labeled for analyses after aligning every configuration to the reference structures. It is shown that these probabilities are all similar for bare CH_5^+, see black bars in Fig. 1, confirming that CH_5^+ remains fully fluxional. This behavior, however, changes dramatically upon microsolvation. Starting with the largest cluster $CH_5^+(H_2)_3$, only three atoms, namely, 1, 2, and 3 according to our labeling scheme, contribute to the moiety, see blue bars. Since atom 2 has twice the probability to participate in the moiety, it can be identified to populate the inner site, whereas atoms number 1 and 3 occupy the outer or in-plane sites. The remaining two atoms exclusively populate the two out-of-plane sites; they are not at all engaged in

scrambling and thus are just "spectators." The important finding is that full hydrogen scrambling in $CH_5^+(H_2)_3$ is stopped entirely at 20 K by freezing the *internal rotation*, which is a direct consequence of microsolvation using three H_2 molecules.

The mechanism responsible for freezing quantum fluxionality is significantly different for $CH_5^+(H_2)_2$, see the green bars in Fig. 1. There, only two atoms, numbers 1 and 2, are found to contribute to the moiety, which is, however, still rotating. This clearly demonstrates that full scrambling is also stopped for $n = 2$, though not by freezing internal rotation as for $n = 3$ but by stopping partial scrambling. Last but not least, $CH_5^+(H_2)$ (red bars) is again similar to the $CH_5^+(H_2)_3$ case.

These qualitatively distinct effects of microsolvation patterns on quantum scrambling are visualized in Fig. 2, in which the diagonal of the nuclear density matrix (which is essentially the square of the nuclear wave function at such low temperatures) is depicted. In $CH_5^+(H_2)_2$, the moiety gets fully localized via the two attached H_2 molecules, whereas the two out-of-plane and the single in-plane atoms yield a ringlike density due to internal rotation of the thus well-defined H_2 moiety with respect to the CH_3 tripod. This is distinctly different for $n = 1$ and 3, where three out of five sites remain coupled via purely quantum-mechanical large-amplitude motion—partial scrambling—thus yielding transiently the H_2 moiety (visualized by the upper three regions of high proton density corresponding to atoms 1, 2, and 3, as labeled in Fig. 1). Contrary to the $n = 2$ species, the two out-of-plane sites remain well localized as spectators in the tripod (thus yielding the two well-defined localization regions corresponding to atoms 4 and 5 in Fig. 1). This reveals pictorially the subtle competition of microsolvation and quantum effects that leads to different localization patterns and thus structures depending on n.

Quantum localization [32].—In order to quantify the effects of microsolvation on the quantum delocalization properties of the protons, we computed their spreads in $CH_5^+(H_2)_n$, $n = 0, 1, 2, 3$, at 20 K. The radius of gyration, $(\sum_i(\mathbf{r}_i - \mathbf{r}^c)^2/P)^{1/2}$ with $\mathbf{r}^c \equiv \sum_i \mathbf{r}_i/P$ serves as our measure, where $\mathbf{r}_i$ denote the bead positions. For bare CH_5^+, see Fig. 3 Panel A, the distributions of the radii of gyration are extremely broad and similar for all protons, indicating that they are delocalized as expected for the quantum fluxional ground state. This picture changes significantly upon microsolvation with a single H_2 molecule in Fig. 3 Panel B. Not only does the proton, to which the H_2 molecule is attached, become extremely localized (red), but all protons become substantially more localized than in bare CH_5^+. When the second H_2 molecule is attached, see Fig. 3 Panel C, the two protons to which the two H_2 are bound become much more confined (red and yellow) than the three others, which is a clear indication, in terms of quantum localization, that structural subunits are induced upon microsolvation. Interestingly, attaching the third H_2 molecule again yields a nearly uniform distribution for all five protons, see Fig. 3 Panel D. Thus, the localization properties of the protons in the CH_5^+ core are found to critically depend on the number of microsolvating H_2 species, which themselves are not affected in terms of their (de)localization properties (see dashed lines in Fig. 3).

Quasiclassical structure.—The analysis performed so far revealed that the H_2 moiety is on average (de)localized between three or two sites for the $n = 1, 3/n = 2$ species leaving the open question of the presence of the

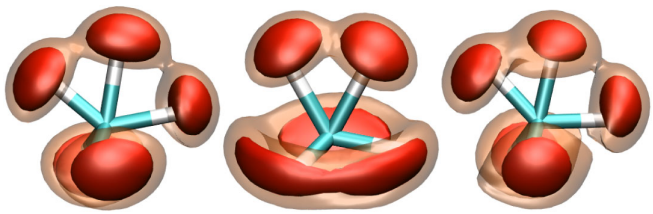

FIG. 2 (color online). Diagonal part of the protonic nuclear density matrix of the CH_5^+ core molecule in 3D space of $CH_5^+(H_2)$ (left), $CH_5^+(H_2)_2$ (middle), and $CH_5^+(H_2)_3$ (right). The solid and transparent isosurfaces correspond to 25% and 10% of the maximum density, respectively. The orientation and thus the site labeling is that of the insets of Fig. 1; i.e., the H_2 moiety corresponds to the upper two or three regions of high proton density and the bonds are only drawn to guide the eye for easy comparison.

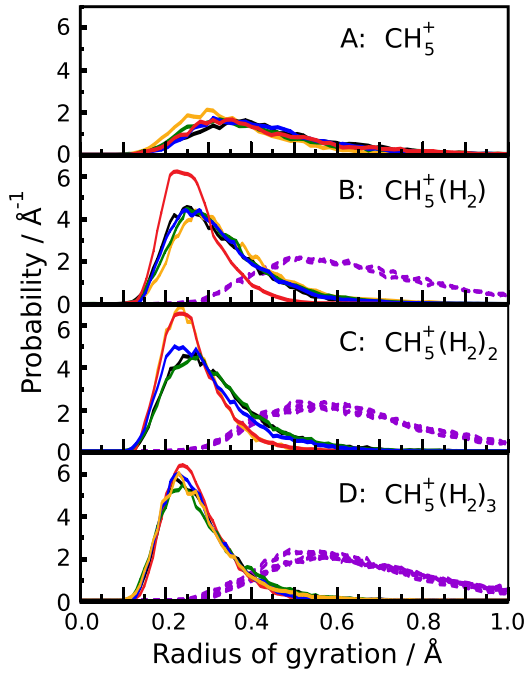

FIG. 3 (color online). Radii of gyration for the five protons in the CH_5^+ core (solid lines) of bare CH_5^+ (Panel A), $CH_5^+(H_2)$ (Panel B), $CH_5^+(H_2)_2$ (Panel C), and $CH_5^+(H_2)_3$ (Panel D), and for the protons in the microsolvating H_2 molecules (dashed lines).

instantaneous quasiclassical structures. To address this point, we computed all those atom pairs that form the moiety for each bead in each path configuration along the trajectories. Then values $x = \max_1(i, j)/P$, where $\max_1(i, j)$ is the number of beads that exhibit the most abundant moiety pair out of all (i, j) pairs in a path configuration, were determined and the respective probabilities were computed for all microsolvation complexes, $n = 0$–3. These probabilities, $W(x)$, shown in Fig. 4 as solid lines, reveal dramatic differences between bare CH_5^+ and all microsolvated species, as well as between the cases $n = 1, 3$ versus $n = 2$. Note that in the two limiting cases, namely, when the moiety remains perfectly localized at any pair of sites or if it is equally delocalized between any two possible pairs of sites, $W(x)$ would be a delta function at 1.0 and 0.5, respectively. In fact, delocalization between two pairs of sites is equivalent to the delocalization between three sites, as the two pairs must have one site in common in view of the nature of the underlying partial scrambling mechanism. In reality, such limiting behavior is not expected to be seen. However, the cases $n = 1$ and 3 (red and blue lines) yield a significant peak close to 0.5 and feature, therefore, a moiety that is simultaneously delocalized over three sites. The distribution of the $n = 2$ species (green line), in stark contrast, is peaked much closer to unity, and thus its moiety is rather localized involving only two sites. Small contributions below $x = 0.5$ can be attributed to fluctuations, which is in line with the site-specific analysis, see the numbers in Fig. 1, where fluctuations appear to about the same order of magnitude. The corresponding reference of bare CH_5^+ is qualitatively different, with the maximum below 0.5, which indicates a significant amount of fluctuations reflecting its highly delocalized nature and complete absence of structure in the quasiclassical sense.

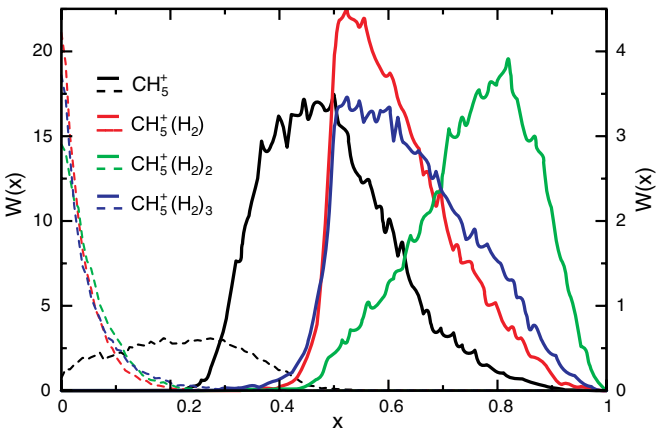

FIG. 4 (color online). Probability densities $W(x)$ for $x = \max_1(i, j)/P$ (solid lines, right scale) and $x = 1 - (\max_1(i, j) + \max_2(i, j))/P$ (dashed lines, left scale), see text, where (i, j) constitute ten possible moiety combinations; note the different scales on the left and right y axes. Color code: bare CH_5^+ $n = 0$ (black), $n = 1$ (red), $n = 2$ (green), and $n = 3$ (blue).

In order to quantify the magnitude of fluctuations for all microsolvation complexes, we calculated x also for the second most represented moiety pair for each path configuration $\max_2(i, j)$ analogously to $\max_1(i, j)$ discussed above (data not shown). The complement of their sum to unity, $x = 1 - (\max_1(i, j) + \max_2(i, j))/P$ directly quantifies the significance of the fluctuations; note that this value is strictly zero if the H_2 moiety is delocalized involving no more than two pairs of sites. The corresponding probability densities, see dashed lines in Fig. 4, clearly show that the fluctuations are by no means small for bare CH_5^+, which again ties back to the fact that the CH_5^+ reference is dominated by large quantum fluctuations. In stark contrast, the fluctuations are similar and minute for all solvated cases, which confirms that the moiety is mostly delocalized over not more than three sites. This also complements the observation that all gyration radii contracted upon adding just one solvating H_2 molecule, see Fig. 3. Overall, this analysis demonstrates that partial scrambling in both $CH_5^+(H_2)$ and $CH_5^+(H_2)_3$ leads to a genuinely quantum-mechanical smearing of the H_2 moiety involving three atoms and three sites, whereas $CH_5^+(H_2)_2$ possesses structure in the quasiclassical sense.

Conclusions and outlook.—In this Letter we demonstrate that microsolvating CH_5^+ by H_2 molecules changes significantly its quantum fluxional motion. At about 100 K, only slowdown of quantum fluxionality is observed, whereas full scrambling is frozen at 20 K due to microsolvation. Most interestingly, there is still partial scrambling possible at 20 K for both $CH_5^+(H_2)$ and $CH_5^+(H_2)_3$, involving the delocalization of only three out of five protons. Complete localization of CH_5^+ in terms of a quasiclassical molecular skeleton consisting of a CH_3 tripod and a well-defined H_2 moiety is induced only when attaching exactly two H_2. This rich scenario is certainly expected to be reflected in many ways in the vibrational spectra of $CH_5^+(H_2)_n$ species. In particular, we predict the presence or absence of the "scrambling peak" at around 750 cm^{-1}, which has been shown [9,14] for bare CH_5^+ to be a unique marker resonance indicating the absence or presence of partial scrambling, to emerge correspondingly for microsolvated $CH_5^+(H_2)_n$. The unraveled competition of microsolvation and quantum effects in molecular aggregates, depending on n and temperature, is a fundamental phenomenon—observable by vibrational spectroscopy—and as such expected to be of broad relevance to many communities.

We are most grateful to Harald Forbert, Stephan Schlemmer, and Oskar Asvany for fruitful discussions. The authors acknowledge partial support by DFG (MA 1547/4), FCI (Chemiefonds-Stipendium to A. W.), RD IFSC, and the Cluster of Excellence RESOLV (EXC 1069) funded by the Deutsche Forschungsgemeinschaft. The simulations were carried out at HLRB München, RV-NRW, and BOVILAB@RUB.

*Present address: Institut für Physik, Universität Rostock, 18051 Rostock, Germany.
sergei.ivanov@uni-rostock.de

[1] T. Oka, Phil. Trans. R. Soc. A **324**, 81 (1988).
[2] G. E. Scuseria, Nature (London) **366**, 512 (1993).
[3] J. S. Tse, D. D. Klug, and K. Laasonen, Phys. Rev. Lett. **74**, 876 (1995).
[4] D. Marx and M. Parrinello, Nature (London) **375**, 216 (1995).
[5] E. T. White, J. Tang, and T. Oka, Science **284**, 135 (1999); for spectrum see http://www.sciencemag.org/feature/data/987367.shl.
[6] D. Marx and M. Parrinello, Science **284**, 59 (1999).
[7] D. Marx and M. Parrinello, Science **286**, 1051 (1999); see Technical Comments at http://www.sciencemag.org/cgi/content/full/286/5442/1051a.
[8] A. B. McCoy, B. J. Braams, A. Brown, X. Huang, Z. Jin, and J. M. Bowman, J. Phys. Chem. A **108**, 4991 (2004).
[9] O. Asvany, P. Kumar, P. B. Redlich, I. Hegemann, S. Schlemmer, and D. Marx, Science **309**, 1219 (2005).
[10] X. Huang, A. B. McCoy, J. M. Bowman, L. M. Johnson, C. Savage, F. Dong, and D. J. Nesbitt, Science **311**, 60 (2006).
[11] X. Huang, L. M. Johnson, J. M. Bowman, and A. B. McCoy, J. Am. Chem. Soc. **128**, 3478 (2006).
[12] X.-G. Wang and T. Carrington, Jr., J. Chem. Phys. **129**, 234102 (2008).
[13] S. D. Ivanov, O. Asvany, A. Witt, E. Hugo, G. Mathias, B. Redlich, D. Marx, and S. Schlemmer, Nat. Chem. **2**, 298 (2010).
[14] P. Kumar P. and D. Marx, Phys. Chem. Chem. Phys. **8**, 573 (2006).
[15] A. Witt, S. D. Ivanov, G. Mathias, and D. Marx, J. Phys. Chem. Lett. **2**, 1377 (2011).
[16] K. Hiraoka and P. Kebarle, J. Am. Chem. Soc. **97**, 4179 (1975).
[17] K. Hiraoka, I. Kudaka, and S. Yamabe, Chem. Phys. Lett. **184**, 271 (1991).
[18] D. W. Boo and Y. T. Lee, Int. J. Mass Spectrom. Ion Process. **159**, 209 (1996).
[19] D. W. Boo and Y. T. Lee, Chem. Phys. Lett. **211**, 358 (1993).
[20] D. W. Boo, Z. F. Liu, A. G. Suits, J. S. Tse, and Y. T. Lee, Science **269**, 57 (1995).
[21] D. W. Boo and Y. T. Lee, J. Chem. Phys. **103**, 520 (1995).
[22] D. Marx and M. Parrinello, Z. Phys. D **41**, 253 (1997).
[23] J. Hutter *et al.*, CPMD, IBM Corp 1990–2008, MPI für Festkörperforschung Stuttgart (1997–2001), http://www.cpmd.org.
[24] D. Marx and J. Hutter, *Ab Initio Molecular Dynamics: Basic Theory and Advanced Methods* (Cambridge University Press, Cambridge, 2009).
[25] E. Fois, A. Gamba, and M. Simonetta, Can. J. Chem. **63**, 1468 (1985).
[26] S. J. Kim, P. R. Schreiner, P. v. R. Schleyer, and H. F. Schaefer, III, J. Phys. Chem. **97**, 12232 (1993).
[27] A. Witt, S. D. Ivanov, H. Forbert, and D. Marx, J. Phys. Chem. A **112**, 12510 (2008).
[28] S. Grimme, J. Comput. Chem. **27**, 1787 (2006).
[29] A. Witt, Ph.D. thesis, Ruhr-Universität Bochum, 2010.
[30] See Supplemental Material http://link.aps.org/supplemental/10.1103/PhysRevLett.110.083003 for benchmarking of the DFT + B + D setup against quantum chemistry reference calculations.
[31] M. P. Deskevich, A. B. McCoy, J. M. Hutson, and D. J. Nesbitt, J. Chem. Phys. **128**, 094306 (2008).
[32] The term "quantum localization" should not be confused with the one from Ref. [11] where it stands for the preferential localization of H versus D in the H_2 moiety of bare CH_5^+.